Blowing bubbles

Icke, V.

Astron. Astrophys. 202, 177–188 (1988)

ASTRONOMY AND ASTROPHYSICS

Blowing bubbles

V. Icke

Sterrewacht Leiden, Postbus 9513, 2300 RA Leiden, The Netherlands

Received August 25, 1987; accepted January 20, 1988

Summary. When an explosion occurs in an inhomogeneous medium, the resulting shock propagates anisotropically. Likewise, a supersonic stellar wind, blowing into such a medium, generates an aspherical cavity. I derive an approximation for the propagation of nonspherical wind-driven bubbles, based on Kompaneets's treatment of a point explosion in an inhomogeneous atmosphere. The partial differential equation that describes such bubbles is separable in the case that the atmosphere, into which the bubble is blown, has been deposited by a previous slow stellar wind. This condition occurs in planetary nebulae, which thus provide an interesting illustration of the mechanism discussed here. In some cases, the same formalism can be applied to bubbles blown by intrinsically nonspherical winds (e.g. due to jets). As an example, this approximation is applied to SS433/W50.

I conclude that: the influence of an external velocity field on the shape of the bubble is usually small; extremely aspherical bubbles are very difficult to form, even if they are driven by sharp jets; accretion disks do not produce very good collimation of a wind from their central object; the inner (reverse) shock that occurs in the wind shares approximately the same asymmetries as the outer shock; and the asymmetry of the inner shock can lead to considerable focusing of the stellar wind.

Key words: hydrodynamics – stars: mass loss – planetary nebulae

1. Introduction

Interstellar holes are often caused by point explosions, such as those due to novae and supernovae; the hydrodynamics of the formation of these holes is well understood (e.g. Zel'dovich and Raizer, 1966). If an explosion occurs in an inhomogeneous medium (Kompaneets 1960), as is almost always the case in the interstellar gas, interesting effects may occur (Icke 1973, Chevalier and Gardner 1974). In recent years, it has become clear that the non-impulsive deposition of energy, for example by a fast stellar wind, leads to another set of remarkable phenomena. The theory of spherical bubbles blown by a supersonic wind is now mature (Castor et al., 1975; Weaver et al., 1977; Kwok, 1982; Lamers 1983; Kahn, 1983), so it seems appropriate to consider the behaviour of nonspherical wind-blown bubbles (cf. Kahn and West, 1985).

In the following, I will concentrate on the shape and flow of such bubbles, assuming that the thermal behaviour of the gas is not too different from the spherical case (see e.g. Lamers, 1983; Kahn, 1983). If a supersonic wind hits an external medium, a shock wave begins to travel into the surrounding gas. The presence of the obstruction ahead is communicated by pressure waves traveling into the wind, which waves pile up due to the motion of the oncoming gas. The "world lines" of these waves in a position-time diagram ("simple waves"; cf. Zel'dovich and Raizer, 1966, Sect. 9) then overlap and form a caustic cusp. This corresponds to the formation of another shock around the source of the wind. Because the jump through this shock occurs in a sense opposite to the outer shock, the inner discontinuity is sometimes called a "reverse" or "excretion" shock.

If the wind is very fast, the jump across the reverse shock is very large, so that the gas behind it is completely subsonic. This means that the pressure waves that communicate the presence of the external obstruction can travel fairly far upstream, so that the inner shock is small compared with the external one. Accordingly, I consider the two shocks as separate entities in Sects. 2, 3, and 4.

In the Kompaneets (1960) approximation, applied to a shock-enclosed bubble that is driven by a continuous wind, the shape of the outer shock is determined by the acceleration parameter A, which is the ratio of the inner pressure over the outer density (it has the dimension of a velocity squared). I present several general solutions for the evolution of such a bubble. These include a do-it-yourself kit for arbitrary functions $A(\theta)$, with which nonspherical shocks can be easily calculated. The solutions are applied to the type of flow expected in planetary nebulae. As a further example, I calculate the shape of a bubble inflated by a highly directional wind from the binary star SS433, and compare the results with the radio bubble W50 that surrounds this enigmatic "jet" source.

2. The Kompaneets approximation for a wind-driven bubble

2.1. *The equation of motion*

Consider a stellar wind, not necessarily isotropic, and its interaction with a surrounding gas cloud. If the wind is fast enough, it will drive a shock into the cloud. In the following, I will assume that radiative effects are not very important in determining the shape of the shock. This assumption is questionable when the shock has propagated for a long time; in that case, radiative cooling will have allowed the gas inside the bubble to collect immediately behind the shock, forming a thin shell. It is known that in the case of a spherical shell, the resulting shock propagation properties are (but for numerical factors close to unity) identical with those in the adiabatic case (Chernyi, 1957; Zel'dovich and Raizer, 1966). In the nonspherical case, the motion of the gas in the thin shell behind the shock has a component transverse to the shock normal (Kahn and West, 1985). This leads

to a somewhat different form of propagation in older nonspherical nebulae.

As long as radiative energy losses are not dominant, the conservation of mass, momentum, and energy impose the familiar jump conditions

$$v_1=\frac{1}{\gamma+1}\,[(\gamma-1)v_0+2s_0^2/v_0], \tag{1}$$

$$P_0+\rho_0 v_0^2=P_1+\rho_1 v_1^2, \tag{2}$$

if the gas streaming through the shock is an ideal gas with adiabatic index γ, and v is the component of the velocity perpendicular to the shock (e.g. Zel'dovich and Raizer, 1966, Ch. I.15). Here s is the adiabatic speed of sound. A subscript 0 indicates the conditions ahead of the shock, and 1 refers to the conditions behind it. If the shock is very strong, that is, if $P_1/P_0 \gg 1$, then Eq. (2) becomes approximately

$$v_0^2=\frac{P_1/\rho_0}{1-\rho_0/\rho_1}=\frac{\gamma+1}{2}\,\frac{P_1}{\rho_0}\equiv K. \tag{3}$$

The above equations are valid in the frame in which the shock is at rest; if the velocity of the external medium is zero, then $-v_0$ is the propagation speed of the shock. But if the cloud into which the shock moves has a velocity u, then the velocity D of the shock obeys

$$v_0=u-D. \tag{4}$$

Because $\boldsymbol{D}$ is always perpendicular to the shock, one finds instead of Eq. (3)

$$D=u_n+\sqrt{K}, \tag{5}$$

for the absolute value D, where u_n is the component of $\boldsymbol{u}$ perpendicular to the shock.

It was first shown by Kompaneets (1960) that Eq. (3) can be solved by separation of variables, in the case that P_1 is constant along the shock surface and ρ_0 is a plane-parallel exponential atmosphere. In the Kompaneets approximation, P_1 decreases in the course of time, because the shock is driven by a single point explosion that deposits a fixed amount of energy into a volume that steadily increases as the shock encompassing it propagates outward. In the case of a steady wind, considered here, P_1 depends only weakly on time. Moreover, I extend Kompaneets' approximation in the sense that I take K to be prescribed, allowing either P_1, or ρ_0, or both, to be a given function of the spatial coordinates.

In what follows, I will assume that the wind comes from a point source, and that the external medium into which the shock is driven has either been deposited by the same source during an earlier phase of mass loss, or owes its form to the gravitational attraction of an object at the origin of the wind. Under these circumstances, it is profitable to express Eq. (5) in spherical coordinates (r, θ, ϕ). I assume cylindrical symmetry, so that all dependences on ϕ vanish. If λ is the angle between $\boldsymbol{D}$ and the radius vector, then (see Fig. 1)

$$u_n=u_r\cos\lambda+u_\theta\sin\lambda, \tag{6}$$

$$\tan\lambda=-\frac{1}{r}\,\frac{\partial r}{\partial\theta}, \tag{7}$$

where u_r and u_θ are the radial and polar components of the velocity in the external cloud, and $r(\theta)$ describes the shape of the

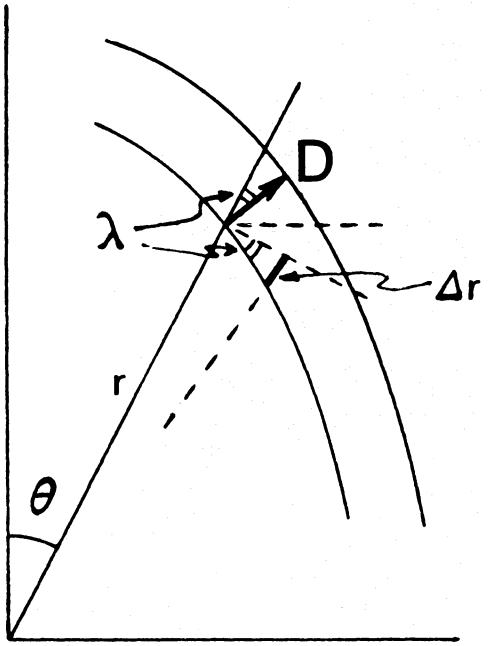

Fig. 1. Geometry of the Kompaneets approximation. Shown is a convex section of the shock, and the same an instant later. The angle λ between the velocity $\boldsymbol{D}$ of the shock and the radius vector also defines the deviation Δr of the shock from spherical symmetry

shock. From Eq. (5) it follows that

$$D=\frac{\partial r}{\partial t}\cos\lambda=u_r\cos\lambda+u_\theta\sin\lambda+\sqrt{K}. \tag{8}$$

Dividing this by $\cos\lambda$ and using Eq. (7) gives

$$\frac{\partial r}{\partial t}=u_r-u_\theta\frac{1}{r}\frac{\partial r}{\partial\theta}+\left\{K\left[1+\left(\frac{1}{r}\frac{\partial r}{\partial\theta}\right)^2\right]\right\}^{1/2}, \tag{9}$$

(cf. Kompaneets, 1960, Eq. (5)). If the external cloud has been produced by an earlier mass loss phase, then $u_\theta=0$, so that

$$\frac{\partial r}{\partial t}=u+\left\{A\left[1+\left(\frac{1}{r}\frac{\partial r}{\partial\theta}\right)^2\right]\right\}^{1/2}, \tag{10}$$

where u now stands for u_r. Moreover, if the preceding mass loss phase was supersonic, then we have approximately

$$\rho_0=(r_0/r)^2\,\rho_*(\theta), \tag{11}$$

so that Eq. (10) becomes

$$r_0\frac{\partial x}{\partial t}=u e^{-x}+\left\{A\left[1+\left(\frac{\partial x}{\partial\theta}\right)^2\right]\right\}^{1/2},$$

$$x\equiv\log r/r_0;\ A\equiv\frac{\gamma+1}{2}\,P_1/\rho_*. \tag{12}$$

Note that the property $P_1/\rho_0 \propto r^{-2}f(\theta)$ makes Eq. (12) *separable* in the case $u=0$. The dependence on the inverse square of the radius occurs in atmospheres that have been deposited by a wind with a constant velocity (e.g. Hippelein et al., 1985) which makes this functional form eminently useful. However, other density distributions (e.g. the more clumpy ones expected in molecular

clouds) can be treated in this approximation by going back to Eq. (10).

2.2. The influence of the external velocity

Now let us consider the function A. Physically, it describes the ratio of the driving force behind the shock to the inertia of the material ahead of it; consequently, the local acceleration of the front is determined by A. Clearly, the shape of the shock is determined by asymmetries of the density ahead of the shock, of the velocity ahead of it, or of the pressure behind it, or a combination of these.

In the Kompaneets case, ρ_0 is an exponential plane–parallel distribution, and it was assumed that the matter enclosed by the shock is so hot that it moves very subsonically with respect to the discontinuity, wherefore P_1 is about constant along the shock. If the bubble is being blown by a wind that is very fast compared with the shock speed, then the temperature beyond the reverse shock is very high. In the hot subsonic bubble that is thereby formed, the constancy of P_1 is a reasonable approximation. In what follows, the ratio P_1/ρ_0 is allowed to vary as a function of the polar latitude. Normally, this variation is then attributed to the behaviour of the external density, but mathematically this does not matter.

Many cosmic high-energy flows show a pronounced double-lobed symmetry, sometimes well collimated into jets; therefore, it is interesting to see if Eq. (12) has straightforward solutions that show the consequences of a medium being blown up by the action of such asymmetric winds, or if there are plausible distributions of the external density ρ_0 that can collimate a spherical wind to form such jets.

First, consider the case where the external density and the internal pressure are spherically symmetric, so that A is constant. Then Eq. (12) can be written in the dimensionless form

$$\frac{\partial x}{\partial \tau} = w e^{-x} + \left(1 + \left(\frac{\partial x}{\partial \theta}\right)^2\right)^{1/2},$$

$$\tau \equiv t\left(A/r_0^2\right)^{1/2}; \; w \equiv u/\sqrt{A}. \tag{13}$$

Evidently, if w deviates a little from spherical symmetry, then the shock propagates faster in the direction where w is largest. Consider the following prescription for w:

$$w = W(1 + \delta \cos 2\theta), \tag{14}$$

which is the lowest-order deviation from spherical symmetry. Two solutions of Eqs. (13, 14), obtained by means of a fixed point explicit numerical difference scheme, are shown in Fig. 2. These and other such solutions show that the shock does not become very aspherical if $W < 1$ and if $\delta < 0.3$; the reason is that the first term on the right hand side of Eq. (13) declines exponentially as the shock progresses. Apparently, only a very strong and very asymmetric streaming in the external gas has a noticeable influence on the shape of the shock. I know of no cases of astrophysical interest in which the matter ahead of the shock shows such pronounced asymmetric motions, except perhaps in the so-called "head-tail" radio galaxies.

Second, consider the case where A is nonspherical, but the wind speed is spherically symmetric. Then u is constant, and the lowest order deviation of A is

$$A = B(1 + \delta \cos 2\theta). \tag{15}$$

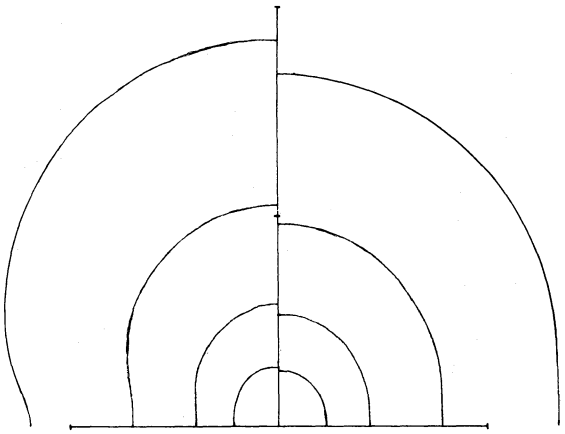

Fig. 2. Propagation of a shock driven by a spherical wind into an atmosphere that has a spherical density distribution and an aspherical radial velocity field. Right: $W = 1.0$, $\delta = 0.2$. Left: $W = 1.0$, $\delta = 0.4$. The shocks are shown at dimensionless times 0.5, 1.0, 1.5 and 2.0. The vertical axis, here and in the following, is the symmetry axis; the horizontal one is the equatorial plane. Tick marks are at intervals $r = 5$

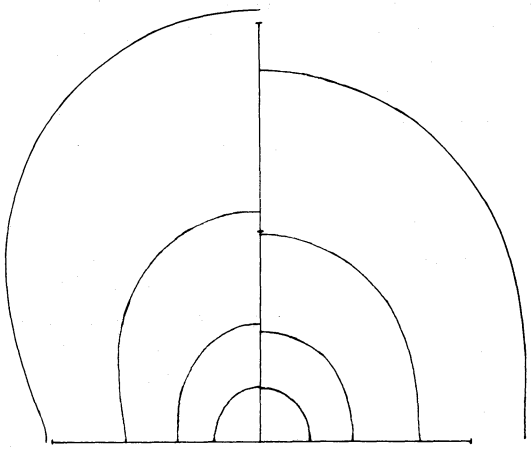

Fig. 3. Propagation of a shock driven by a spherical wind into an atmosphere that has a spherical radial velocity distribution and an aspherical density. Right: $W = 1.0$, $\delta = 0.2$. Left: $W = 1.0$, $\delta = 0.4$. The shocks are shown at dimensionless times 0.5, 1.0, 1.5 and 2.0

In that case Eq. (12) becomes

$$\frac{\partial x}{\partial \tau} = w e^{-x} + \left\{(1 + \delta \cos 2\theta)\left(1 + \left(\frac{\partial x}{\partial \theta}\right)^2\right)\right\}^{1/2}, \tag{16}$$

$$\tau \equiv t/\sqrt{B}, \; w \equiv u/r_0\sqrt{B}.$$

Solutions of Eq. (16), obtained as above, are shown in Fig. 3. Clearly, the asymmetry of A has a more pronounced effect than an equal asymmetry of the external velocity. It appears from a series of similar solutions that the overall shape of the shock hardly depends on w; if $w > 1$, the physical size of the shock is bigger than if $w = 0$, but its geometrical shape is not influenced much.

In some cases, we might expect a situation in which the wind from the central object moves into an oncoming accretion flow. A

series of solutions of this case was calculated as above; I find that only the size of the shock changes markedly, but its shape does not change much.

These calculations appear to establish that the external velocity field matters comparatively little. This is due to the exponential in Eq. (12), which occurs because of the outward decrease in the external density (11) that is imposed by mass conservation. It is not very probable that something very different from (11) would apply (e.g. a constant external density), because it is likely that the surrounding cloud was ejected supersonically. Consequently, I will ignore the external velocity altogether and take $u=0$. In that case, the solutions of Eq. (12) can be obtained in a more systematic way.

2.3. *Construction of the complete integral*

If the external velocty is zero, Eq. (12) becomes

$$\frac{\partial x}{\partial t}=\left\{A(\theta)\left(1+\left(\frac{\partial x}{\partial \theta}\right)^2\right)\right\}^{1/2}, \tag{17}$$

which can be solved by separation of variables. In this way, we obtain a solution, called the complete integral, that depends on a free parameter E and a free function $g(E)$. By constructing the envelope of a family of curves described by this integral (which I will call "partial waves" by analogy with wave propagation), we can obtain all other solutions that conform to a given initial condition (e.g. Courant and Hilbert, Vol. II, Chap. II, par. 4). Assuming now that x is the sum of a function of t and a function of the latitude θ, we find[1]

$$x=Et\pm\int(E^2/A-1)^{1/2}\,d\theta+g(E). \tag{18}$$

If the shape of the initial cavity is given at $t=0$, then $g(E)$ must be chosen in such a way that $x=x(\theta)$ conforms to this initial condition. In the following I will always start with an initial sphere; since $x=\log r/r_0$, we have $x=0$ for all E at $t=0$. Inspection of Eq. (28) shows that this implies that we must take the minus sign before the integral, and $g=0$:

$$x=Et-\int(E^2/A-1)^{1/2}\,d\theta, \tag{19}$$

$$r=r_0\,e^{Et}\exp\left(-\int(E^2/A-1)^{1/2}\,d\theta\right). \tag{20}$$

Only in exceptional cases, such as the one described by Kompaneets (1960), can the integral in Eq. (19) be obtained in closed form. But a numerical quadrature is quite straightforward, and can be executed with arbitrary precision (in all following calculations I will use a five-point Newton-Cotes integration). The advantage of my analytical procedure over a finite-difference solution of Eq. (17) is, that one need not worry about stability. Such worry is very justified, because of the quadratic occurrence of $\partial x/\partial\theta$. A local increase of the slope of x is locally amplified, and clearly when the point $\partial x/\partial\theta=1$ is approached, the nonlinearity will generate runaway "solutions".

Underlying these instabilities is a genuine physical effect. If $\partial x/\partial\theta$ is locally large, then x will increase rapidly with time. Consequently, any region where $x(\theta)$ is steep will propagate to adjacent regions. This has a profound influence on the shape of the cavity enclosed by the shock. For example, suppose that $A(\theta)$ is very large in a narrow zone (say ten degrees) around $\theta=0$, as might happen in a cavity formed by a well collimated jet. Then initially we will see a bubble with a steep gradient near $\theta=10°$, but as time goes on this region propagates towards the equatorial plane $\theta=\pi/2$. Thus, *a very narrow jet will not always form a very narrow cavity*[2] (examples of this will be given below).

The evolution of the shock is calculated as follows. First, determine the function A in Eq. (3):

$$A=\tfrac{1}{2}(\gamma+1)\,P_1/\rho_0. \tag{21}$$

By choosing the time scale, this function can always be normalized such that the maximum value of A is 1, as inspection of Eq. (17) shows. For example, let

$$A\equiv\delta+(1-\delta)\exp(-\theta^2/\sigma^2). \tag{22}$$

Second, calculate the integral

$$T\equiv-\int(E^2/A-1)^{1/2}\,d\theta, \tag{23}$$

for a suitable range of allowed values of E. In this example, A decreases monotonically from 1 to approximately δ (unless $\sigma\simeq\pi/2$), so that $\sqrt{\delta}\lesssim E\leqq 1$. Because $\partial x/\partial\theta=0$ at $\theta=0$ and approximately at $\theta=\pi/2$, this implies (via Eq. (17) that

$$x=e^t \quad \text{(along the symmetry axis)}, \tag{24}$$

$$x=e^{t\sqrt{\delta}} \text{ (in the equatorial plane)}. \tag{25}$$

Obviously, the axial ratio H of the cavity enclosed by the shock evolves according to

$$H=e^{t(1-\sqrt{\delta})}. \tag{26}$$

A series of curves $T(E)$ is plotted in Fig. 4, in the case $\sigma=40°$, $\delta=0.5$.

Third, construct the envelope for the required value of t. From the solution (19) we see that the envelope at $t=0$ is the envelope of all solutions $T(E)$; inspection of Fig. 5 shows that this envelope is the line $x=0$, which yields $r=r_0$ in Eq. (20), as it should be. At later times, say $t=2$, an easy graphical way to obtain the envelope solution is as follows. Trace the first "partial wave" $T(1)$ on a transparency. Then shift this up over a distance $(1-E)t$ for the next value of E (in this example, $E=0.95$ and $t=2$, so the shift is 0.1), and trace the corresponding $T(E)$. Do this for all E (see Fig. 5). Draw the envelope of this set of curves; this is $x(t,\theta)$, the "wave front" that is tangent to all partial waves. Solutions for $t=0.5$, 1, 2 and 3 are given in Fig. 6. Since $r=r_0e^x$, a graph of the cavity shape $r/r_0=\exp x(t,\theta)$ can be obtained immediately (Fig. 7).

[1] If Eq. (11) does not hold, for example if the external density is a constant, then the separation in Eq. (18) changes. As can be seen from Eq. (10), the square root in Eq. (17) acquires a factor e^{-x}, and the time coordinate is determined by an integration (as in the Kompaneets case).

[2] This may become more intuitively evident if you consider such a cavity as being due to two supersonic bullets moving in opposite directions. Their Mach cones meet in the equatorial plane, creating a cavity that, in projection, has a diamond shape. Such shapes are seen in planetary nebulae, in the radio source W50, and maybe in some nebulae around Wolf-Rayet stars.

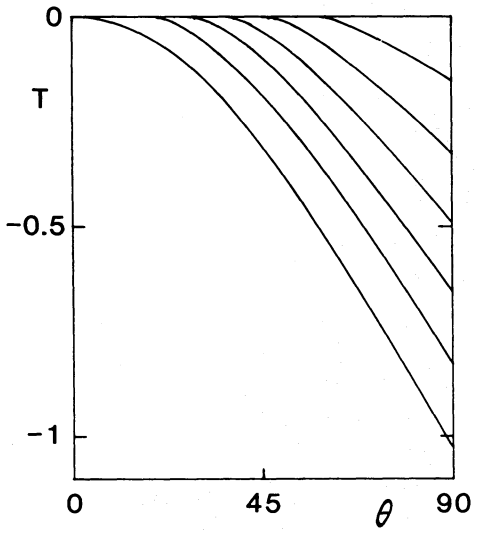

Fig. 4. Complete integral $T(E,\theta)$ in the case $\sigma=40°$, $\delta=0.5$. Values of E are: 1 (lower curve), 0.95, 0.9, 0.85, 0.8, 0.75 (upper curve)

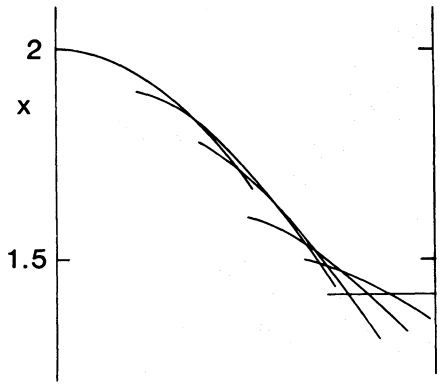

Fig. 5. Partial waves derived by shifting the complete integrals $T(E,\theta)$ by an amount $(1-E)\,t$, for $t=2$. The envelope of these sections is the solution for the shock propagation at that time, and is shown as the third curve in Fig. 6

3. Applications of the formalism

3.1. Non-spherical winds: SS433/W50

The above construction is a very rapid, convenient, and physically meaningful way to estimate the consequences of asphericities inside or outside a wind-driven bubble. Using this generalized Kompaneets approximation, I have constructed propagating shocks for a few dozen different distributions $A(\theta)$. It turns out that, if A is symmetric about the equatorial plane, the resulting shock cross section almost always develops into a rather plump figure 8, somewhat like two touching spherical bubbles (cf. Königl 1982, 1983). Only if A has regions of very steep dependence on the latitude θ do the bubbles become strongly aspherical. The cause for this was mentioned above. In particular, *the wind from a star that is surrounded by an accretion disk is not well collimated by the presence of the disk.* If the disk itself provides extra aspherical pressure, for example due to evaporation, the collimation could be much better (V. Icke and S.-U. Choe, unpublished). In that

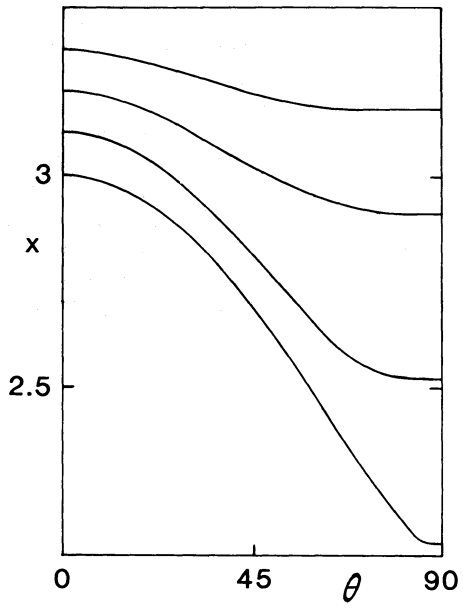

Fig. 6. Solution $x(t,\theta)$ obtained by forming envelopes of the complete integral. Values of t are: 0.5 (top curve), 1.0, 2.0 and 3.0 (bottom curve). Ordinate values refer to the bottom curve; ordinates for the other curves must be shifted so that $x(0.5, 0)=0.5$, $x(1, 0)=1$, and $x(2, 0)=2$

case, the dynamical pressure in the external medium can be included in the acceleration function A; however, the discussion on the influence of the external velocity in the previous paragraph indicates that a rather large external dynamic pressure would be needed.

Likewise, *a narrow jet does not necessarily create a very narrow cavity.* In some cases, such as in extragalactic radio sources, and

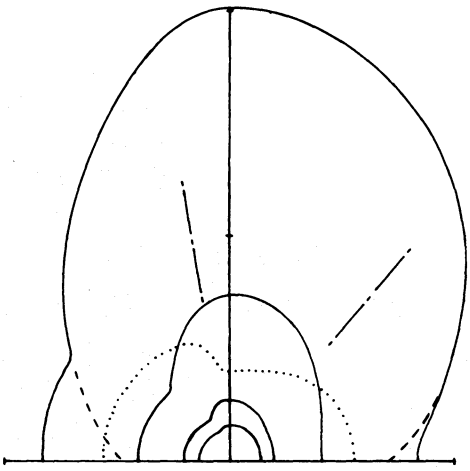

Fig. 7. Propagation of a shock driven by a spherical wind into a stationary atmosphere that has a nonspherical density distribution. Right: $\sigma=40°$, $\delta=0.5$. Left: $\sigma=10°$, $\delta=0.5$. Dimensionless times are 0.5, 1, 2, and 3. Distance to tick marks is $r=10$. A density contour is shown as a dotted line. The opening angle σ is shown by a dot-dashed line. The shape of the partial wave due to the asymmetry alone is shown by a dashed line; for large times, the solution tends to this cusped shape. The same solutions are obtained if the external medium is spherically symmetric, but the wind is asymmetric (see text). In that case, σ is the opening angle of the asymmetric part of the wind

especially in the binary star SS433 and its surounding radio source W50, there are jets blowing bubbles (Zealey, et al., 1980; Beer and Pounds, 1981; Margon, 1984). A fast jet blowing a bubble falls within the Kompaneets approximation for the following reason. If the shock is caused by a single very strong explosion, as in the Kompaneets case, the temperature behind the shock is very high, so that motions inside the shock bubble are very subsonic. This allows P_1 in Eq. (3) to be constant along the shock, and the shock shape is due to asphericities in the outside density ρ_0. However, if the jet is very supersonic, the transverse pressure wave caused by it propagates only very slowly compared with the main stream of the jet. Then we may – to first approximation – add a term $P_1(\theta)$, describing the dynamic pressure of the jet, to a spherically symmetric pressure component. In that case we will get an aspherical cavity, even if ρ_0 is spherically symmetric. The above approach uses the fact that the cavity shape is determined exclusively by the acceleration A, which is proportional to the *ratio* P_1/ρ_0 of the inside/outside conditions.

The results in Fig. 7 are examples of this; Fig. 8 shows some more, in the case where the spherical component of the internal pressure is less important. It appears immediately from these calculations that the characteristic diamond shape of W50 is approximated by the early stages of a narrow jet piercing an initially spherical shock, shown on the left hand side of Fig. 7. However, if we assume that the shape of W50 is due to the jets of SS433, we must take into account that these jets, which individually are only 4° wide, precess on a cone with half-angle 20° (e.g. Hjellming and Johnston, 1981; Margon, 1984). Consequently, it would seem to be more accurate to use a conical beam:

$$A=\delta+(1-\delta)\exp-\{(\theta-20°)/4°\}^2. \tag{27}$$

The best fitting solution of this sort has $\delta=0.5$ and $\tau=1.5$ (Fig. 9). But the fit is very unsatisfactory; although the radio contours at higher flux density show something of a double bump straddling the axis of the source (Geldzahler et al., 1980), the lower contours delineate a spindle shape that is not reproduced at all by assuming the hollow conical distribution in Eq. (27). Projection effects are known to be present because the axis of the cone traced by the jets is inclined 80° with respect to the line of sight (Margon, 1984), but the deviation of only 10° from the perpendicular is small enough that such effects are negligible.

It turns out that a single-jet distribution like (22) fits W50 better than the conical jet (27) (Fig. 10); the best fit for δ is 0.5, and for σ I obtain about 10°. It is remarkable that this fits better than $\sigma=20°$, which is the value one might at first want to use because of the SS433 geometry.

Although it is risky to draw conclusions on the basis of the shape of W50 alone (to begin with, the velocity field is not known),

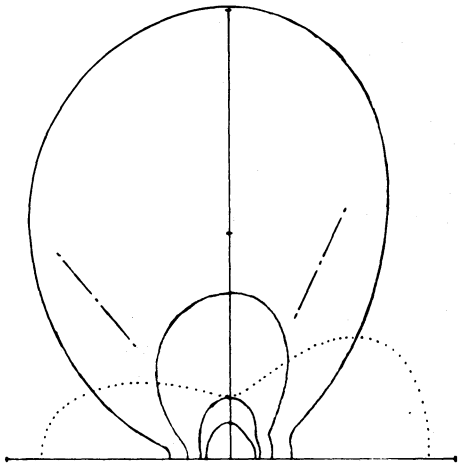

Fig. 8. As Fig. 7, for $\sigma=40°$, $\delta=0.1$ (left) and $\sigma=25°$ (right)

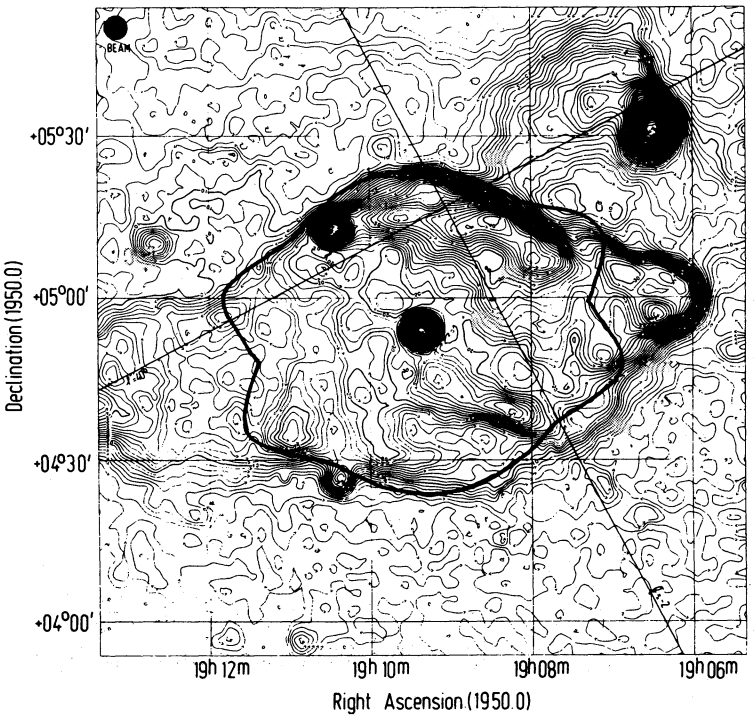

Fig. 9. Best fit to the radio source W50 of a cavity blown by the precessing jets of SS433. The shape of the cavity is superimposed on the 2695 MHz map of Geldzahler et al., (1980)

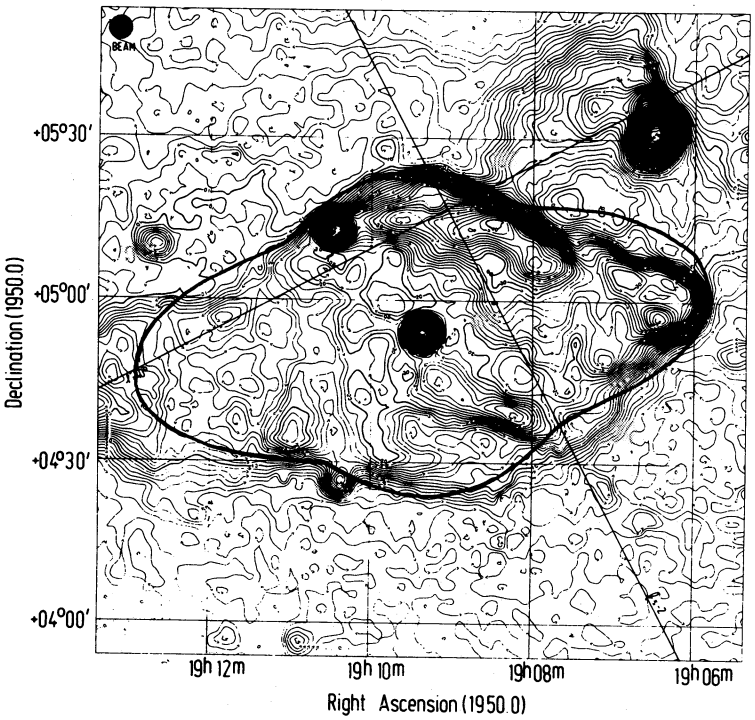

Fig. 10. Best fit to the radio source W50 of a cavity blown by a gaussian jet with width $\sigma = 10°$. The spherical sections near the equatorial plane require a fairly large isotropic pressure component in addition to the jets, so that $\delta = 0.5$. Evidently, this fit is very bad; it is interesting to note that this shape is a rather good fit to the "homunculus" of η Carinae

it would appear from the above that, at large distances from SS433, the gas of the jets blends with other material, perhaps the very gas that has been ejected along the jets before. *The hollow precession cones are thereby changed into a pair of filled-center cones*, with an opening half-angle of about 10°. It is tempting to identify the region where this filling-in occurs with the location where the extended X-rays originate (Margon, 1984); other possible interactions of the gas emitted by SS433, such as might take place in the "brightening zone" inferred by Vermeulen et al. (1987), do not seem to destroy the collimation immediately. In any case, the narrowness of the bumps on the W50 "lemon" is *prima facie* evidence for recollimation of the jets far from the central source.

If we accept the above fits to the W50 cavity, we can deduce the following. Adopting a distance of 5.5. kpc (Hjellming and Johnston, 1981), we have that one parsec at the source corresponds to 0.'63 as seen from Earth. The scaling of Figs. 9 and 10 then implies $r_0 = 4.1\ 10^{16}$ m for the hollow cone, and $r_0 = 3.5\ 10^{16}$ m for the filled center beam. The dimensional time scale can be retrieved from the dimensionless one by

$$t = \tau r_0^2 \left(\frac{\gamma+1}{2} \frac{P_1 r_0^2}{\rho_*} \right)^{-1/2}. \tag{28}$$

Now the jet force $P_1 r_0^2$ is roughly given by

$$P_1 r_0^2 = L/v = 10^{24}\ \mathrm{N}, \tag{29}$$

where L is the jet power and v its speed (cf. Hjellming and Johnston, 1981). Using $n_* = 10^8\ \mathrm{m}^{-3}$, or $\rho_* = 2\,10^{-19}\ \mathrm{kg\,m}^{-3}$, and $\gamma = 5/3$, I obtain

$$t = 3.9\,10^{-22}\ \tau r_0^2\ \mathrm{s}. \tag{30}$$

Because $\tau = 1.5$ for the hollow cone and $\tau = 2$ for the solid one, I find in both cases that

$$t = 9.6\,10^{11}\ \mathrm{s} = 3\,10^4\ \mathrm{yr}, \tag{31}$$

which corresponds fairly well to the age of W50 as estimated by Begelman et al. (1980); see also Königl (1982, 1983).

3.2. *Planetary nebulae*

The current consensus model of planetary nebulae holds that the appearance of their luminous shells is due to the interaction between a stellar wind and the remnant of an older red giant envelope. The envelope was presumably deposited during a mass loss episode when the progenitor star went through the so-called Mira and OH/IR phases on the asymptotic giant branch. At some point, the star switches from a comparatively dense slow wind ($10\ \mathrm{km\,s}^{-1}$) to one that is tenuous and very fast (up to $2000\ \mathrm{km\,s}^{-1}$). The momentum densities in these winds are comparable, but the velocity difference implies that the fast wind blows a shock-enclosed bubble into the envelope (which, for practical purposes, can be considered static). A reverse shock then propagates into the fast wind (Weaver et al., 1977; Lamers, 1983; Kahn, 1983; Kahn and West, 1985).

The envelope has a density that decreases roughly as r^{-2} (cf. Hippelein et al., 1985), so the formalism of Sect. 2.3 should apply very well to planetary nebuale. If the slow wind produces a mass loss $\dot{M}$ with speed w, we have

$$\rho_0 w r^2 = \dot{M}/4\pi = \text{constant}, \tag{32}$$

so that

$$\rho_0 = (r_0/r)^2\ \dot{M}/(4\pi\ w\ r_0^2) \equiv (r_0/r)^2\ \rho_*(\theta). \tag{33}$$

Defining the dimensionless acceleration and time by

$$A \equiv \frac{\gamma+1}{2} \frac{P_1}{\rho_0} r_0^{-2} \equiv \frac{\gamma+1}{2}\ V^2\ r_0^{-2}\ h(\theta), \tag{34}$$

$$\tau \equiv t \left(\frac{\gamma+1}{2}\ V^2\ r_0^{-2} \right)^{1/2}, \tag{35}$$

the equation of motion (17) takes the form

$$\partial x/\partial\tau = \{h(\theta)\,[1+(\partial x/\partial\theta)^2]\}^{1/2}. \tag{36}$$

The velocity $\boldsymbol{D}$ of the outer shock then has the components (in cylindrical coordinates (r, z))

$$(D_r, D_z) = \sqrt{h(\theta)}\,[\sin(\theta+\lambda), \cos(\theta+\lambda)], \tag{37}$$

$$\lambda = -\arctan(\partial x/\partial\theta). \tag{38}$$

Separation of variables in Eq. (36) gives as before

$$x = E\tau - \int (E^2/h(\theta)-1)^{1/2}\,d\theta. \tag{39}$$

This equation allows us to prove a remarkable fact, namely that *the shock evolves towards a fixed shape in a finite time*; after that time, the shock changes only by expanding with a constant scale factor. This can be seen most easily if $h(\theta)$ is a simple decreasing function of θ. The allowed values of the separation constant E are then bounded by

$$E_0 \equiv \sqrt{h(0)} \geq E \geq \sqrt{h(\pi/2)} \equiv E_1. \tag{40}$$

When $E = E_0$, the integral spans a range between zero and the maximum value

$$I_{\max} = \int_0^{\pi/2} (E_0^2/h-1)^{1/2}\,d\theta = \int_0^{\pi/2} (h(0)/h(\theta)-1)^{1/2}\,d\theta. \tag{41}$$

At the other extreme, $E = E_1$, the integral is identically zero; this corresponds to the partial wave that generates a spherical shock, i.e. the initial conditions. This partial wave propagates according to

$$x_1 = E_1\tau, \tag{42}$$

for all values of θ, whereas the partial wave corresponding to the value E_0 (this is the fastest-moving partial!) obeys

$$\begin{aligned} &x_0 = E_0\tau \text{ at } \theta = 0, \\ &x_0 = E_0\tau - I_{\max} \text{ at } \theta = \pi/2. \end{aligned} \tag{43}$$

As the graphical construction in Figs. 4, 5, and 6 shows, this implies that the propagation of the fastest partial wave always wipes out the initial conditions in a finite time. Thus, the shock changes shape until the time

$$\begin{aligned} \tau_{\text{crit}} &= I_{\max}/(E_0 - E_1) \\ &= \left(\sqrt{h(0)} - \sqrt{h(\pi/2)}\right)^{-1} \int_0^{\pi/2} \left[\frac{h(0)}{h(\theta)} - 1\right]^{1/2} d\theta, \end{aligned} \tag{44}$$

after which *the shape of the shock remains the same*, except for a global scale factor. This behaviour has important consequences for the observations of internal motions in planetary nebulae (Icke et al., 1988; Icke and Preston, 1988).

As can be seen from the graphs in Fig. 4, the partial wave integrals typically do not have a zero derivative in the equatorial plane $\theta = \pi/2$. Thus, the ultimate shape of the shock has a *cusp* at its equator (see Fig. 7 and examples below). It is not clear that this situation can persist; if it does, an interesting flow pattern must be expected, because shocks that converge at an acute angle produce sharp jets emanating from the cusp, by means of the "shaped-charge" mechanism (Batchelor, 1974, Sect. 6.3).

A plausible functional form of the density distribution in the envelope of a planetary nebula is

$$h(\theta) = \delta + (1-\delta)\,\exp[\tfrac{1}{2}\sigma(\cos(2\theta)-1)]. \tag{45}$$

Examples of shocks propagating in such atmospheres, for various combinations of δ and σ, are shown in Figs. 11 and 12. It is immediately evident that even very disk-like envelopes do not produce very good collimation. However, there is encouraging agreement with shock shapes observed in young planetaries (Reipurth, 1987), in intermediate ones (Okorokov et al., 1985) and in older "butterfly" types (Balick, 1987a, b; Balick and Preston 1987; Balick et al., 1987; see also Sabbadin, 1984, and references therein).

From calculations like these one can derive the velocities one expects to observe in spectroscopic observations of planetary nebulae. The theoretical models correspond rather precisely to the observations of the so-called "spindle" or elliptical planetaries (Balick et al., 1987). Likewise, the "butterfly" types can be easily explained (Icke et al., 1988), provided that the density contrast between the equator and the poles of the envelope is large. It is at present wholly unknown how such an envelope is deposited, but there is no doubt that they exist (e.g. Torrelles et al., 1983).

4. The inner shock

If a supersonic wind hits some external gas, two shock waves are formed: one that travels into the surrounding envelope, and one that goes upstream into the wind. The fact that there is an obstruction ahead is communicated by pressure waves travelling into the wind. These waves pile up at caustic cusps in the phase plane of the flow, thereby forming the upstream-facing shock that surrounds the wind source. This reverse shock (also called "excretion shock" or "standoff shock") must become asymmetric if the envelope into which the fast wind blows is not spherical. The acceleration of the outer shock is anisotropic; we have seen above how that leads to the formation of an aspherical outward facing shock. Since the pressure waves must travel further if the outer shock is far from the wind source, I expect that *the inner shock is aspherical in the same sense as the outer shock.*

The inner shock is much smaller than the outer one (Kahn, 1983). The pressure waves that travel upstream from the outer shock move in a very hot medium, where the speed of sound is not strongly dependent on the position. Thus, throughout the nebula, the news that there is an obstruction ahead travels almost the same distance upstream in a given time interval, and to first approximation the position of the reverse shock is then a fixed distance away from the outer shock. This implies that the asphericities of the outer shock are amplified; in the cases considered above, the inner shock is expected to have an approximately prolate shape about the axis of symmetry.

In stellar winds, the flow enclosed by the inner shock is presumably spherically symmetric. In such a case, the flow meets an oblique shock except possibly at the equator and at the poles. I will assume that the inner shock deviates only to first order from a sphere:

$$\left(\frac{1}{a}\cos\theta\right)^2 + \left(\frac{1}{b}\sin\theta\right)^2 = 1/r^2, \tag{46}$$

which is an ellipsoid. Because of the applications considered here, it is taken to be prolate: $b/a < 1$. The following analysis can of course be carried out for any other convex cylindrical shape.

The angle β between the radius (which is the direction of the incoming flow) and the local tangent of the ellipse obeys

$$\beta = \theta + \arctan(b^2/a^2\tan\theta). \tag{47}$$

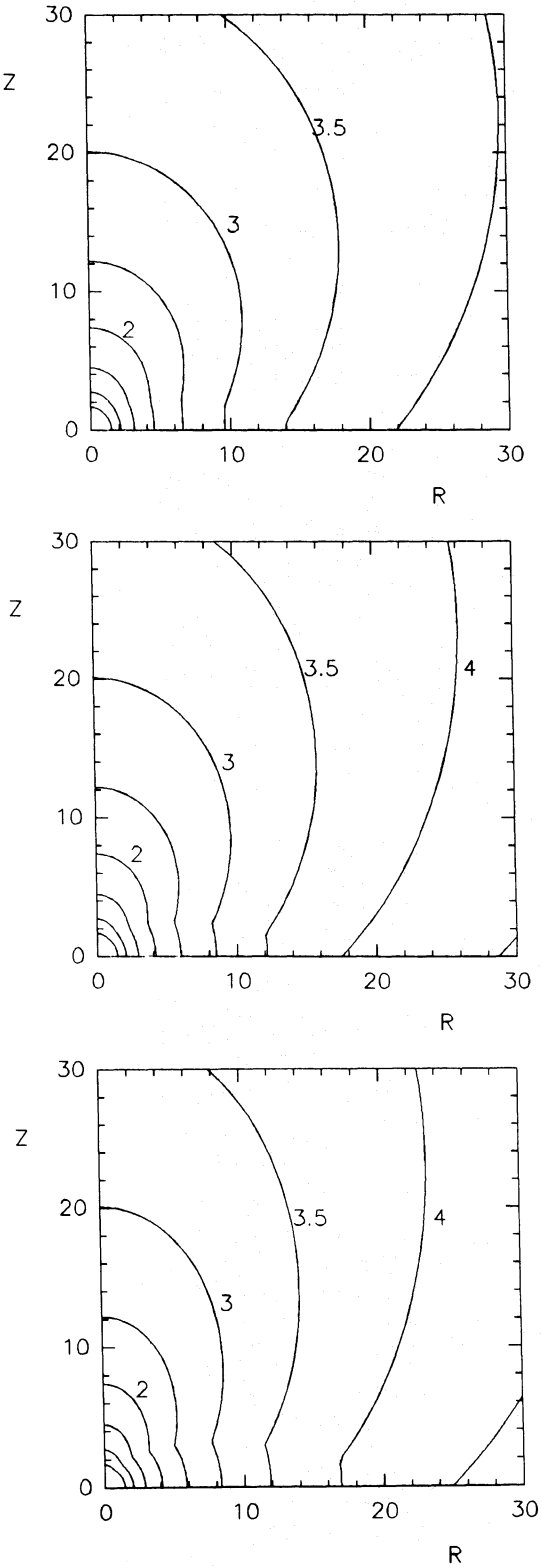

Fig. 11. Models of the evolution of the outer shock in planetary nebulae. The envelope density is described by Eq. (45) in the case $\delta = 0.5$ and $\sigma = 2$, 4, and 8 (top to bottom panels). Dimensionless times of the shock positions are 0.5, in steps of 0.5, to 3. The symmetry axis is at the left edge of each frame, the symmetry plane at the bottom edge. Notice the appearance of an equatorial cusp at dimensionless time $\tau = 3.76$, 3.99, and 4.39 (from top to bottom)

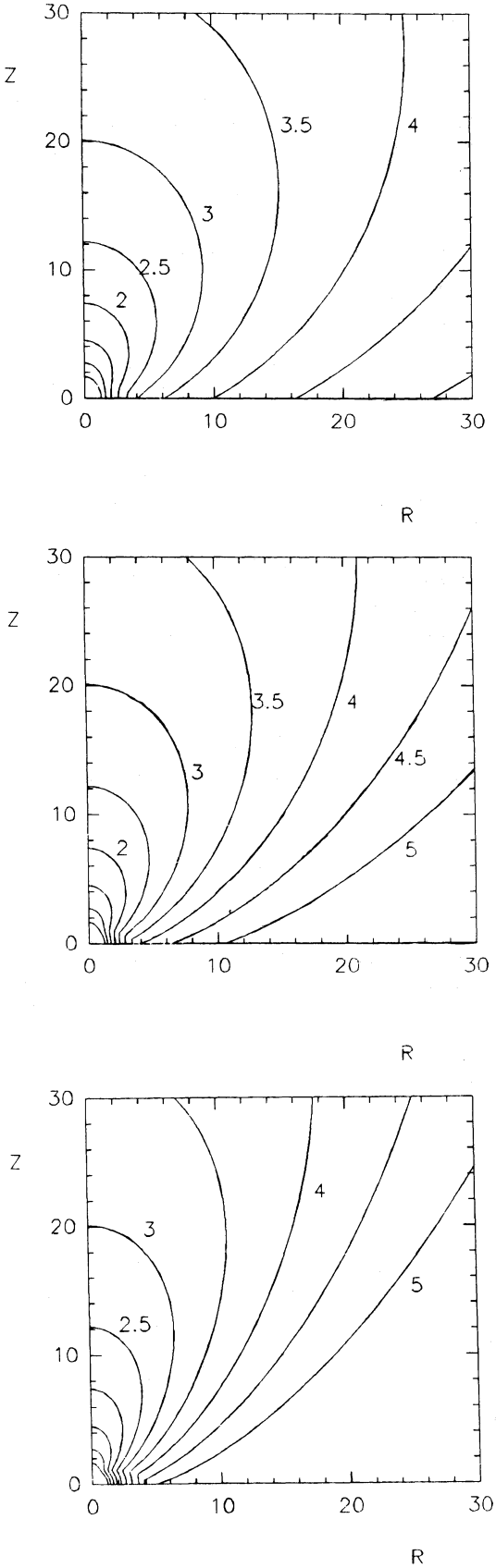

Fig. 12. As Fig. 11, but for $\delta = 0.1$. Equatorial cusps appear at $\tau = 3.23$, 4.01, 4.95

This has a maximum at

$$\theta_m = b/a. \tag{48}$$

At that point, the shock is most oblique, and therefore near $\theta = \theta_m$ interesting things may occur. For example, if the value of β (say β_m) corresponding to θ_m is smaller that the local Mach angle, no shock occurs at all:

$$\sin \beta_m < \sin A = 1/M_0, \tag{49}$$

where M_0 is the Mach number of the incident flow. Because of Eqs. (47, 48) we get

$$M_0 < \tfrac{1}{2}(a/b + b/a), \tag{50}$$

for the no-shock condition, independently of the adiabatic index. It is to be expected that this will not usually be fulfilled; for example, if the temperature of the stellar wind is 10^5 K and if it moves with 2000 km s^{-1}, then $M_0 \approx 70$. Unless the axial ratio b/a is improbably small[3], there will be a shock even at θ_m (note that the large value expected for M_0 justifies the approximation that the inner shock is stationary, as will be assumed in the following). But even if there is a shock, the obliquity near θ_m will cause it to be weaker, and therefore the postshock speed will be larger and the temperature jump smaller.

Assuming the incoming flow to be an ideal gas with polytropic index γ, so that

$$P = \rho s^2/\gamma = \kappa \rho^\gamma;\ e = s^2/\gamma(\gamma-1) = \frac{kT}{m(\gamma-1)}, \tag{51}$$

one obtains, using the jump conditions across an oblique shock at angle β,

$$v_{1\perp} = \frac{s_0}{\gamma+1}\{(\gamma-1)M_0 \sin\beta + 2/M_0 \sin\beta\}, \tag{52}$$

$$v_{1\parallel} = v_{0\parallel} = s_0 M_0 \cos\beta. \tag{53}$$

Here s is the speed of sound; an index 0 indicates a variable before passage through the shock, while an index 1 refers to the situation after. The density, pressure, and energy density obey the familiar relations

$$s_1 = s_0(\gamma+1)/\{(\gamma-1) + 2/M_0^2 \sin^2\beta\}, \tag{54}$$

$$P_1 = \frac{P_0}{\gamma+1}\{2\gamma M_0^2 \sin^2\beta - (\gamma-1)\}, \tag{55}$$

$$e_1 = \frac{e_0}{(\gamma+1)^2}\{2\gamma M_0^2 \sin^2\beta - (\gamma-1)\}\ \{(\gamma-1) + 2/M_0^2 \sin^2\beta\}. \tag{56}$$

Unless b/a is exceedingly small, we do not expect β to be too far from 90°. Then we can take the limit $M_0 \to \infty$, in which case

$$v_{1\perp} = \left(\frac{\gamma-1}{\gamma+1}\right) s_0 M_0 \sin\beta = \left(\frac{\gamma-1}{\gamma+1}\right) v_0 \sin\beta = \left(\frac{\gamma-1}{\gamma+1}\right) v_{0\perp}, \tag{57}$$

$$v_{1\parallel} = s_0 M_0 \cos\beta = v_0 \cos\beta = v_{0\parallel}, \tag{58}$$

$$\rho_1 = \frac{\gamma+1}{\gamma-1}\rho_0, \tag{59}$$

$$P_1 = P_0 \frac{2\gamma}{\gamma+1} M_0^2 \sin^2\beta, \tag{60}$$

$$e_1 = e_0\left(\frac{\gamma-1}{\gamma+1}\right)^2\left(\frac{2\gamma}{\gamma-1} M_0^2 \sin^2\beta - 1\right). \tag{61}$$

The angle ψ of the direction into which the gas is deflected with respect to the local tangent at θ is

$$\tan\psi = v_{1\perp}/v_{1\parallel} = \{(\gamma-1)M_0 \sin\beta + 2/M_0 \sin\beta\}/(\gamma+1)M_0 \cos\beta, \tag{62}$$

$$\tan\psi = \left(\frac{\gamma-1}{\gamma+1}\right)\tan\beta. \tag{63}$$

The angle χ by which the incoming stream is deflected is clearly

$$\chi = \beta - \psi. \tag{64}$$

Using Eq. (63) we get

$$\tan\chi = \frac{2\tan\beta}{(\gamma+1) + (\gamma-1)\tan^2\beta}, \tag{65}$$

and, because of Eq. (47),

$$\tan\beta = (\tan\theta + b^2/a^2 \tan\theta)/(1 - b^2/a^2). \tag{66}$$

Because of the ellipticity of the shock, the distance from $r = 0$ to the discontinuity is not constant, so that the value of M_0 at the front is a function of θ. If the flow from the central object is radial, we have from mass conservation that $\rho v r^2 = \dot{M}/4\pi = \text{constant}$. Combining this with Bernoulli's Equation and the equation of state (51), we get

$$A\rho^{\gamma-1} + B/\rho^2 r^4 = 1, \tag{67}$$

with constant A and B. Since we are on the highly supersonic branch of this equation, A is negligible, and we have the usual

$$\rho_0 \propto r^{-2}. \tag{68}$$

Since $e \propto s^2 \propto \rho^{\gamma-1}$, we get

$$e_0 \propto r^{2-2\gamma}, \tag{69}$$

$$M_0 \propto s_0^{-1} \propto r^{\gamma-1}. \tag{70}$$

The radius r follows from Eq. (46) as

$$(b/r)^2 = \frac{b^2}{a^2}\cos^2\theta + \sin^2\theta \equiv R(\theta). \tag{71}$$

If we call ρ, e, and M the values of the mass density, energy density, and Mach number just before the shock on the minor axis, we obtain

$$\rho_0/\rho = R(\theta);\ e_0/e = R^{\gamma-1};\ M_0/M = R^{-(\gamma-1)/2}. \tag{73}$$

Using Eq. (72), we are now able to calculate Eqs. (57–64) as a function of the latitude θ. I have plotted the relevant functions in Fig. 13 for $M = 20$ and $b/a = 0.8$, 0.5 and 0.3. The corresponding postshock velocity vectors in the case $b/a = 0.5$ are shown in Fig. 14.

It is clear that the obliquity along the shock ellipse leads to strong focusing at the major axis (Eichler, 1982). A refracted velocity vector points towards the major axis if $\chi > \theta$. Near the major axis, θ is small; expansion of Eqs. (47, 62, 64) to first order in θ gives

$$\beta = \pi/2 + (1 - a^2/b^2)\theta, \tag{74}$$

[3] Consequently, extremely elongated cavities like those proposed in some models of bipolar nebulae (e.g. Schwartz, 1983, p. 227) could not possibly be surrounded by a closed shock.

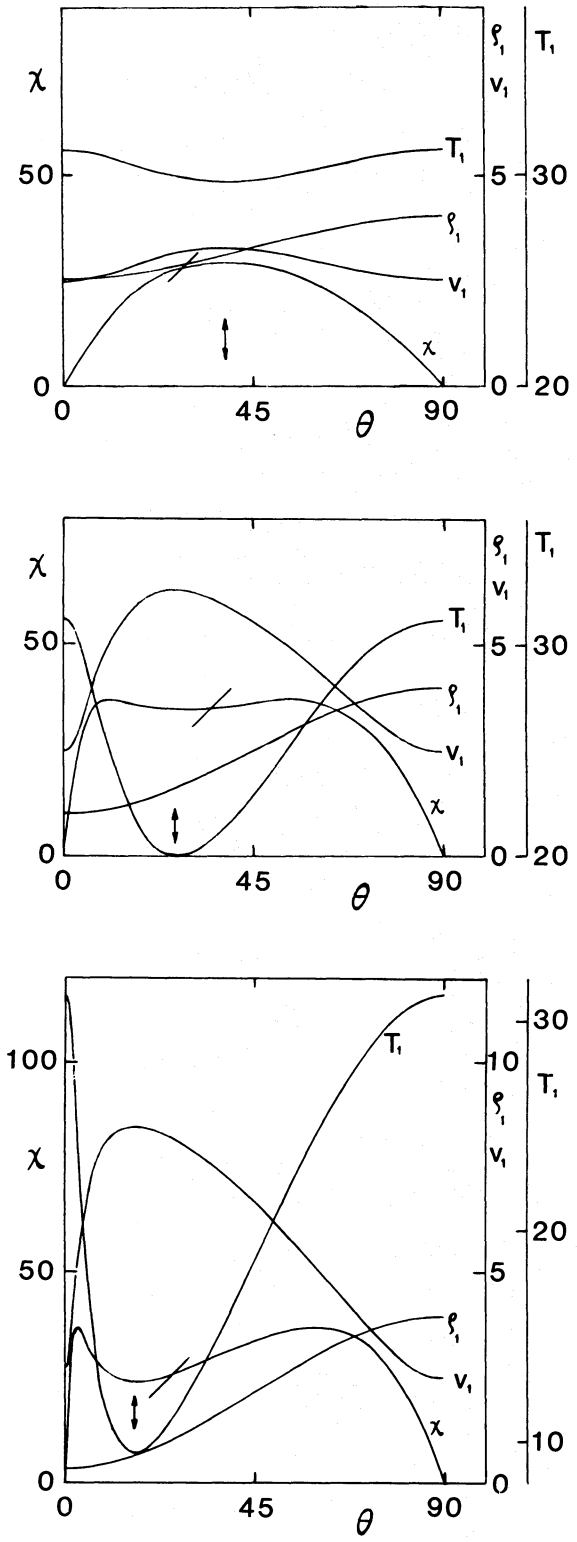

Fig. 13. Deflection angle χ, density ρ_1, speed v_1, and temperature T_1 after passage through an elliptical shock, as a function of the latitude θ of the ellipse. The quantities ρ_1, v_1 and T_1 are expressed in terms of their preshock values on the minor axis; the Mach number there is 10, and $\gamma=5/3$. The steeper part of the ellipse ($\theta=\theta_m$) occurs at the double arrow; for values of θ below those where $\chi=\theta$ (diagonal line) the velocities are focused towards the major axis. (a) axial ratio $b/a=0.8$; (b) $b/a=0.5$; (c) $b/a=0.3$

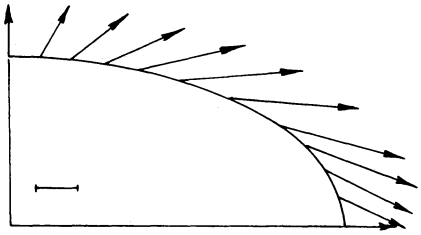

Fig. 14. Velocity vectors after passage through the inner shock. The preshock Mach number is 10, the magnitude of the preshock sound speed is indicated by a bar

$$\psi=\pi/2+(\gamma+1)\,(1-a^2/b^2)\theta/\{(\gamma-1)+2/M_0^2\}, \tag{75}$$

$$\chi=(a^2/b^2-1)\,(2-2/M_0^2)\theta/\{(\gamma-1)+2/M_0^2\}. \tag{76}$$

The condition $\chi>\theta$ then leads to the requirement

$$M_0^2>2\,[2-(\gamma+1)\,b^2/a^2]^{-1}$$

$$b^2/a^2<2(1-1/M_0^2)/(\gamma+1). \tag{77}$$

At $\gamma=5/3$, a value of $M_0=10$ gives focusing for $b/a=0.862$; if $M_0\to\infty$, we have $b/a=\frac{1}{2}\sqrt{3}$. Evidently, *at the high preshock Mach numbers expected here, even a very small eccentricity causes considerable focusing along the major axis.* From Eqs. (47, 63, 64) we see that the condition $\chi=\theta$ for large M_0 is fulfilled at $\theta=\theta_f$, where

$$\tan^2\theta_f=\frac{1}{\gamma-1}\frac{b^2}{a^2}\,(2-(\gamma+1)b^2/a^2). \tag{78}$$

For all $\theta>\theta_f$, the incoming stream is refracted by the shock through such a large angle that the velocity vector points toward the major axis. We note in passing from Eq. (78) that (i) no focusing occurs for $b^2/a^2>2/(\gamma+1)$; (ii) θ attains a maximum value given by $\tan^2\theta_f=1/(\gamma^2-1)$ at $b^2/a^2=1/(\gamma+1)$. Consequently, when $\gamma=5/3$, *the largest fraction of the stellar wind is focused along the major axis if the axial ratio is about* 0.6 (Fig. 15).

The consequences of the focusing are difficult to ascertain without calculating the flow in the entire bubble in great detail. Numerical hydrodynamics appears unavoidable for this. But it seems probable from the above that the collimation of outflow along the symmetry axis is helped by prolateness of the inner shock (additional cooling may help too; cf. Eichler, 1982). There

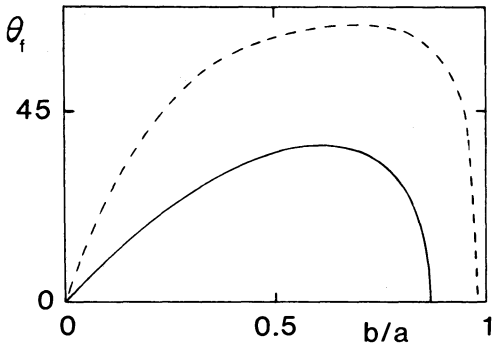

Fig. 15. Latitude θ_f below which axial focusing occurs through the inner shock, versus the axial ratio b/a of the shock ellipse. Full drawn curve is for $\gamma=5/3$, dashed curve is for $\gamma=1.1$

are configurations, such as a spherical wind source in the centre of an evaporating disk, where the inner shock is manifestly elliptical due to the density distribution around the source (V. Icke and S.-U. Choe, unpublished); in such cases, jet collimation is comparatively easy.

5. Concluding remarks

Provided that the thermal behaviour of nonspherical wind-blown bubbles is similar to that of spherical ones, the above shows that:

(i) The influence of an external velocity field on the behvaiour of a bubble is usually marginal.

(ii) A large family of useful solutions for the propagation of nonspherical bubbles can be derived through a simple integration involving the acceleration function $A(\theta)$ which is the ratio of the internal pressure over the external density.

(iii) Only such $A(\theta)$ as have a very steep dependence on the latitude θ produce strongly aspherical cavities.

(iv) In particular, accretion disks do not produce a very sharply peaked $A(\theta)$ and hence do not collimate the wind very well.

(v) Even very narrow jets, corresponding to very sharply peaked $A(\theta)$, will not usually produce a narrow cavity.

(v) If the outer shock is aspherical, so is the inner one, and roughly in the same sense; if the inner shock is prolate along the symmetry axis, the wind from the central source is focused along that axis.

(vii) The formalism presented here is not good enough for planetary nebulae which are so old that radiative effects dominate the propagation of the outer shock and lead to the formation of a thin shell behind the shock. This stage is best investigated by means of numerical hydrodynamics including radiative transfer; a program to do this is under way.

Acknowledgements. This work was begun and mostly completed during Bruce Balick's sabbatical at Sterrewacht Leiden, 1983–1984. I am deeply indebted to him for countless conversations on the subject of this paper, for his patient tutoring on the intricacies of planetary nebula research, and for constant gentle prodding to prepare my results for publication. A visit to the University of Washington at Seattle finally crystallized the work. I thank the referee for some cautionary remarks on the importance of radiative effects. I convey my gratitude to the Leids Kerkhoven-Bosscha Fonds for travel support; to Bruce Balick and Heather Preston for their stimulating collaboration in confronting my models with the observations; and to Frances Verter for spirited discussions of the many aspects of bubbles and for a critical reading of an earlier version of this manuscript.

References

Balick, B.: 1987a, *Sky Telesc.* **73**, 125.
Balick, B.: 1987b, *Astron. J.* **94**, 671
Balick, B., Preston, H.L.: 1987, *Astron. J.* **94**, 958
Balick, B., Bignell, C.R., Hjellming, R.M., Owen, R.: 1987, *Astron. J.* **94**, 948
Balick, B., Preston, H.L., Icke, V.: 1987, *Astron. J.* **94**, 1641
Batchelor, G.K.: 1974, *An Introduction to Fluid Dynamics*, Cambridge Univ. Press
Beer, P., Pounds, K.: 1981. *Vistas Astron.* **25**, Nos. 1 and 2
Begelman, M.C., Sarazin, C.L., Hatchett, S.P., McKee, C.F., Arons, J.: 1980, *Astrophys. J.*, **238**, 722
Castor, J., McCray, R., Weaver, R.: 1975, *Astrophys. J.* (*Letters*), **200**, L107
Chernyi, G.G.: 1957, *Dokl. Akad. Nauk SSSR* **112**, 213
Chevalier, R.A., Gardner, J.: 1974, *Astrophys. J.* **192**, 457
Courant, R., Hilbert, D.: 1968, *Methoden der mathematischen Physik*, Springer, Berlin
Eichler, D.: 1982, *Astrophys. J.*, **263**, 571
Geldzahler, B.J., Pauls, T., Salter, C.J.: 1980, *Astron. Astrophys.* **84**, 237
Hippelein, H.H., Baessgen, M., Grewing, M.: 1985, *Astron. Astrophys.* **152**, 213
Hjellming, R.L., Johnston, K.J.: 1981, *Astrophys. J. Letters* **246**, L141
Icke, V.: 1973, *Astron. Astrophys.* **26**, 45
Icke, V., Preston, H.L.: 1988, *Astron. Astrophys.* (in press)
Icke, V., Preston, H.L., Balick, B.: 1988 (preprint)
Kahn, F.D.: 1983 in: *Planetary nebulae*, D.R. Flower (ed.), Reidel, Dordrecht, p. 305
Kahn, F.D., West, K.A.: 1985, *Monthly Notices Roy. Astron. Soc.* **212**, 837
Königl, A.: 1982, *Astrophys. J.* **261**, 115
Königl, A.: 1983, *Montly Notices Roy. Astron. Soc.* **205**, 471
Kompaneets, A.S.: 1960, *Dokl. Akad. Nauk SSSR* **130**, 1001
Kwok, S.: 1982, *Astrophys. J.* **258**, 280
Landau, L.D., Lifschitz, E.M.: 1966, *Lehrbuch der Theoretischen Physik VI: Hydrodynamik*, Akad. Verlag, Berlin
Lamers, H.J.G.L.M.: 1983, in *Diffuse matter in galaxies*, J. Audouze (ed.), Reidel, Dordrecht, p. 35
Margon, B.: 1984, *Ann. Rev. Astr. Astrophys.* **22**, 507
Okorokov, V.A., Shustov, B.M., Tutukov, A.V., Yorke, H.W.: 1985, *Astron. Astrophys.* **142**, 441
Reipurth, B.: 1987, *Nature* **325**, 787
Sabbadin, F.: 1984, *Astron. Astrophys. Suppl. Ser.* **58**, 273
Schwartz, R.D.: 1983, *Ann. Rev. Astron. Astrophys.* **21**, 209
Torrelles, J.M., Rodriguez, L.F., Cantó, J., Carral, P., Marcaide, J., Moran, J.M., Ho, P.T.P.: 1983 *Astrophys. J.* **274**, 214
Van den Heuvel, E.P.J.: 1981, *Vistas Astron.* **25**, 95
Vermeulen, R.C., Schilizzi, R.T., Icke, V., Fejes, I., Spencer, R.E.: 1987, *Nature* **328**, 309
Weaver, J., McCray, R., Castor, J., Shapiro, P., Moore, R.: 1977, *Astrophys. J.* **218**, 377
Zealey, W.J., Dopita, M.A., Malin, D.F.: 1980, *Monthly Notices Roy. Astron. Soc.* **192**, 731
Zel'dovich, Ya. B., Raizer, Yu. P.: 1966, *Physics of Shock Waves and High-temperature Hydrodynamic Phenomena*, Academic Press, New York